WAVE PHENOMENA IN HELICON PLASMA

V. F. Virko, G. S. Kirichenko and K. P. Shamrai
Institute for Nuclear Research, NAS of Ukraine, Kiev

Employing of the electrodeless, low-pressure inductive discharges (ICPs) is preferable in many applications. A helicon discharge, which is known as the most efficient magnetized ICP [1], operates with excitation of electromagnetic helicon waves (whistlers) obeying the dispersion relation $\omega = \omega_{ce} k_z k c^2 / \omega_{pe}^2$ where ω_{pe} and ω_{ce} are the electron plasma and cyclotron frequencies, and $k = (k_z^2 + k_\perp^2)^{1/2}$ is the total wave number. In a radially bounded plasma, the wave fields vary as $\exp[i(k_z z - \omega t - m\theta)]$ where m is the azimuthal wavenumber. Helicons are excited by external rf antennas of various designs and propagate into plasma giving rise to various wave phenomena that considerably affect the discharge operation. Some of these phenomena are examined below experimentally and theoretically.
PACS: 52.35.-g

1. CAVITY MODES

Helicon waves in short devices are excited as discrete, axially standing modes (i.e., the cavity modes). As the helicon wavelength depends on density, these *geometrical* resonances result in a non-monotonic dependence of the absorbed power on plasma density, with maxima related to excitation of particular modes. However, it is difficult to reveal such dependence in discharge where the density establishes in a self-consistent way. For this reason, we conducted modeling experiments on absorption of a weak rf signal in independently prepared plasma whose density could be varied *ad arbitrium* [2].

The left part of experimental device (see Fig. 1) was a helicon source: a 14 cm diam quartz tube placed in magnetic field about 100 G and excited by an rf antenna made of two straight rods and a connecting ring. It generated a transverse rf magnetic field and thus excited the first (m = 1) azimuthal mode of helicon waves. A 13.56 MHz, 1 kW generator supplied the antenna in a continuous regime. The right part of the device in Fig. 1 is an auxiliary plasma source based on an ECR discharge driven by a pulsed 2.45 GHz magnetron. Two schemes of experiment were used: (1) ECR plasma at low rf power input from the antenna, and (2) helicon discharge at normal rf power. Experiments were done with Ar gas at pressures 0.5–5 mTorr.

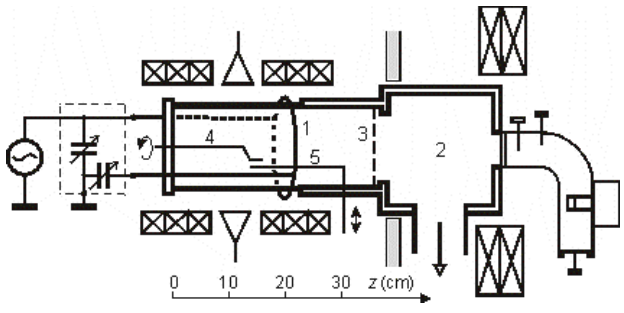

Fig. 1. A schematic of the device. 1 – rf antenna; 2 – ECR chamber; 3 – separating grid; 4 and 5 – probes

In the first scheme, the plasma density in the quartz chamber raised up to some maximum and then fell down to zero during the magnetron pulse. The absorption of the low-power rf signal in the antenna circuit, which was measured by a directional coupler, shows a few resonances at some specific, *resonance* densities. These resonances arise from the excitation of standing modes, as was revealed by measurements with magnetic probes. The resistance of a plasma load is shown in Fig. 2 as a function of density.

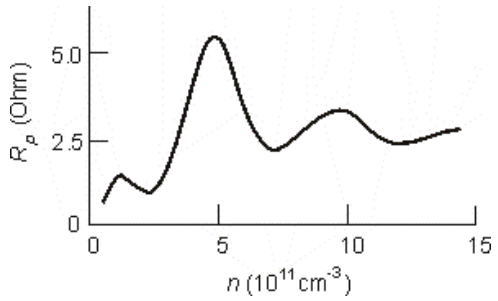

Fig.2. Plasma resistance vs density, for a straight m=1 antenna; p_{Ar} = 0.7 mTorr, and B_0 = 115 G

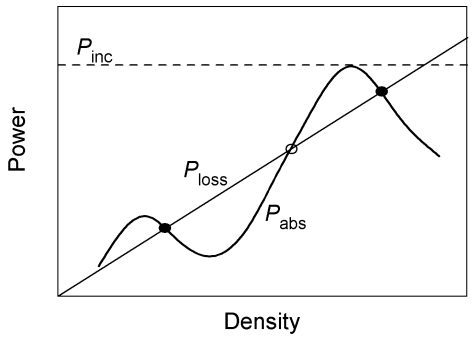

Fig. 3. Schematic diagram of the absorbed power and power loss vs density

The influence of absorption resonances on the discharge behavior is illustrated in Fig. 3. There the absorbed rf power is schematically shown along with the power loss from plasma, which is proportional to density. The power balance constrains the discharge to intersection points. However, at the middle point the equilibrium is unstable. Maximum absorbed power (dashed line) is the total power delivered by generator. If the power decreases, the upper intersection disappears and the discharge must jump to lower density. On the contrary, with increasing power the lower intersection vanishes and the discharge jumps to higher density [3].

Experiments with a stimulated helicon discharge seem to argue for this speculation. Figure 4 shows oscillograms of the rf power absorbed in the ECR plasma when the magnetron pulse is ending and density is decreasing. At low rf power, one can see two absorption maxima at some resonance densities. With increasing rf power, an additional ionization appears and absorption resonances become saw-shaped. If the rf power is high enough, after the end of the ECR pulse a self-sustained helicon discharge arises. Notable is that it can exist in several discrete states with densities that are close to resonance densities. Depending on power the jumps between these states can occur. This result is consistent with observations of the cavity modes in other experiment [4].

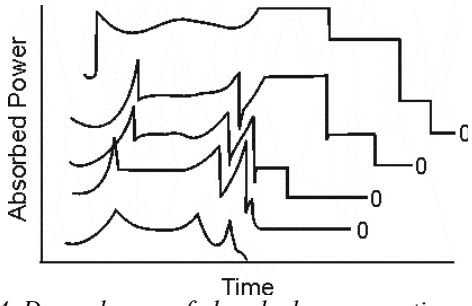

Fig. 4. Dependences of absorbed power on time, at increasing forward rf power

A similar effect occurs when the external magnetic field varies at a fixed rf power. From dispersion relation it follows that the helicon wavelength is proportional to B_0/n. As boundary conditions fix the wavelength of standing mode, the resonance density is proportional to the magnetic field. Thus, with increasing magnetic field the absorption curve in Fig. 3 moves to the right. At some critical magnetic field, it slips out from under the loss line and the discharge jumps to lower density. From Fig. 3, it is also clear that the reflected power (the distance between the discharge point and the incident power line, P_{inc}) becomes zero just before the break off. This effect was really observed experimentally: with increasing B_0 the density grows while reflected power goes to zero, and then the discharge disruption occurs [5].

The values of critical magnetic field and stable densities are determined by the shape of absorption curve. The latter strongly depends, among other factors, on the antenna dimensions and position. An obvious and experimentally confirmed result is that if the antenna length is equal to the wavelength, or if the antenna mid-plane coincides with a node of the standing wave, the corresponding resonance cannot be excited because actions of different antenna parts compensate each other [2,6].

Matching network, which transforms the antenna impedance to the generator output, can strongly deform the absorption curve. It is clear that if matching conditions are adjusted to low, non-resonance plasma resistance, then at the resonance, when the resistance is maximum, bad matching results in that the absorbed power is minimum rather than maximum.

Using the above technique, we compared relative efficiencies of various antennas. Twisted antennas [7] gave identical absorption characteristics because standing helicon wave rotates only in time and has not spatial helicity. Fields from a phased antenna with right-hand rotation (m=+1) penetrate deeply into plasma and maximize in resonance conditions. At left rotation (m=–1), the field do not penetrate to the plasma center. The excitation with a single-loop, azimuthally symmetric m=0 antenna differs from the m=1 excitation. It shows neither distinct absorption resonances nor standing helicon waves, contrary to theoretical prediction [3] and for still unclear reason.

2. ION ACOUSTIC TURBULENCE

Another important problem is how the helicons transfer their energy to plasma. The matter is that the helicons themselves are weakly damped waves. They are low sensitive to collisions because their energy is concentrated in magnetic fields rather than in the particle motion. The real damping is found to be orders of magnitude more than calculated from the binary collisions.

For explanation of the anomalous helicon absorption several linear mechanisms were proposed, such as Landau damping [8] and linear conversion of the helicons in short-scale Trievelpiece-Gould modes [9]. Unfortunately, none of them was directly confirmed or rejected in experiments. Formerly, anomalous helicon absorption was observed in experimental conditions that are strongly different from those considered here [10,11]. It was attributed to the excitation of short ion-sound waves. Recently, it was theoretically assumed that parametrically excited ion-acoustic turbulence might be responsible for the helicon absorption in a helicon discharge as well [12]. Indeed, ion- acoustic waves were detected in the helicon discharge by a microwave scattering technique [13]. We employed probe technique to examine the low frequency oscillations in our device.

Two shielded probes shown in Fig. 1 were used for the interferometry. One of them (marked 4 in Fig. 1) was movable azimuthally at a distance of 5.5 cm from the axis while another (5) in the radial direction across the plasma column. Signals from the probes were added by a mixing circuit and forwarded to the spectrum analyzer.

In the helicon discharge the rf probe reveals a wide noise spectrum of plasma potential oscillations peaking in the low frequency range as well as around harmonics of the pumping frequency (Fig. 5). The amplitude of side-band oscillations near the fundamental frequency is comparable with that at low frequencies (LF) and can even exceed the potential oscillations at the pumping frequency itself.

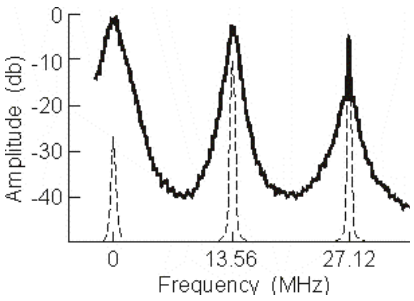

Fig. 5. The spectrum of potential oscillations

The noise arises as a result of combined action of the rf field and the external magnetic field only. It is extremely low in the ECR plasma at zero rf power as well as in inductive discharge driven by the same antenna, but without magnetic field. In this latter case, the spectrum is shown by the dashed lines in Fig.6.

With increasing magnetic field the noise is excited in a threshold manner. The threshold on the rf power, was measured with use of the ECR plasma as seen from Fig. 6.

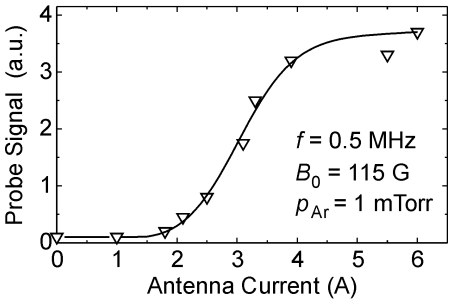

Fig. 6. Noise amplitude vs antenna rf current

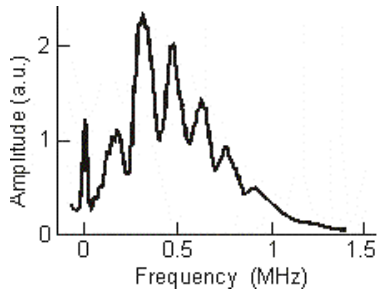

Fig. 7. Interferometric signal from two probes

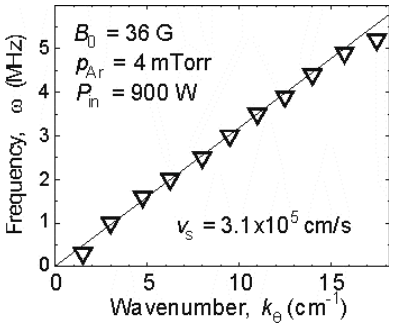

Fig. 8. Dispersion of the LF oscillations

At lower magnetic fields, the noise demonstrates a fair correlation in the azimuthal direction. In Fig. 7, the frequency spectrum is shown of a joint signal from two probes separated by d=2 cm in the azimuthal direction. Considering that the phase velocity is $v_{ph} \approx d\Delta f$ where Δf is the frequency distance between neighboring maxima, one can determine the dispersion (Fig. 8). The phase velocity is found to be constant over the frequency range and to coincide with the ion-acouistic speed, at electron temperature of 4 eV. Varying the gas pressure we compared electron temperatures measured by the Langmuir probe with those calculated from the phase velocities. A good agreement proved that the observed oscillations are really the ion-acoustic waves. They were found to propagate azimuthally in the direction of electron gyration, which coincides with the right-hand helicon rotation (m=+1). With increasing pressure the noise amplitude rapidly decreases.

In contrast with the azimuthal correlation, the radial correlation of oscillations is quite short. In Figs. 10a and 10b the azimuthal and radial spatial correlation functions are plotted at the same frequency and low magnetic field. It is with increasing magnetic field the azimuthal correlation rapidly vanishes.

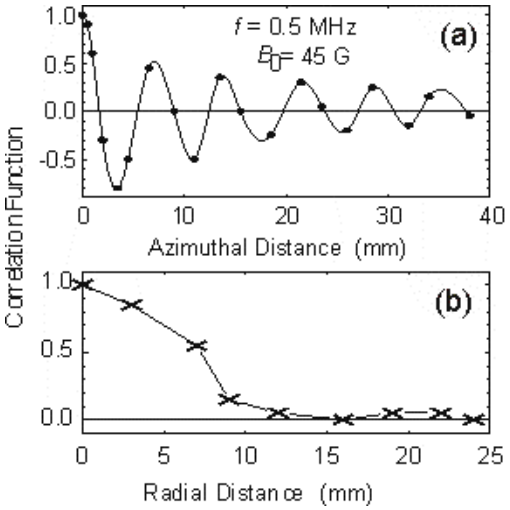

Fig. 9. Azimuthal (a) and radial (b) correlation functions for the LF oscillations.

Two excitation mechanisms most conform with the azimuthal propagation of ion acoustic waves. The first is the parametric instability driven by the rf field. Measurements have shown that along the axis the maxima of the noise amplitude correlate with maxima of the B_z-field of standing m=1 helicon wave. This fact says in favor of the parametric excitation in the inner plasma regions, as long as the B_z field is produced only by transverse rf currents.

The origin for parametric instability; i.e. electron drift relative to ions is characterized by oscillatory electron velocity, $\mathbf{u}$, or by electron excursion, $\boldsymbol{\xi} = \mathbf{u}/\omega$. These values were estimated for specific experimental conditions with use of the computation code based on linear cold-plasma theory [2]. Figure 10 shows the distribution of the azimuthal velocity in cross-section of the plasma column computed for the parabolic density profile at z = 25 cm and for 1 A current in antenna shown

in Fig. 1. The peaks seen in peripheral regions underneath

Fig. 10. Contour plot of u_θ in plasma cross-section (flank circles show the positions of antenna legs)

the antenna legs are due to intense electrostatic fields excited via mode conversion of helicon waves into Trivelpiece-Gould waves at strong density gradient. Peak positions correlate with measured maxima of the LF oscillations. Even at 1 A antenna current, the peaks in Fig. 10 are high enough, $u_{\theta\, max} \approx 0.035 v_{Te}$. The appropriate amplitude of electron azimuthal excursion is of the order of Larmour radius. At maximum antenna currents available in our experiments, 20–30 A, the oscillatory velocity can amount to thermal electron velocity, v_{Te}.

To compute the dispersion of the LF oscillations in helicon plasma, several simplifying assumptions can be made. First, considering very small scales of the LF waves, one can neglect the plasma and pumping field nonuniformities. Next, one can use the potential approximation. Indeed, estimations show that the main part of the side-band spectrum has to be electrostatic rather than helicon waves. Then one can use the dispersion relation for LF oscillations [14], in which parametric effects are determined by the parameter $a_E = \mathbf{k} \cdot \boldsymbol{\xi}$ where $\mathbf{k}$ is the LF wave number. In calculations, the excitation of LF oscillation, Ω, as well as of two side-band satellites near the fundamental frequency, $\Omega \pm \omega_0$, was included whereas the effect of higher harmonics was neglected. In Fig. 11, an example is shown of the dispersion computed for some typical experimental parameters; $\cos\varphi = 0.042$ where φ is an angle between $\mathbf{k}$ and $\mathbf{B}_0$; and $u = 0.05 v_{Te}$. With increasing k; i.e. with increasing a_E the nonlinearity first appears as the shift of $\mathrm{Re}\Omega$ above the ion-acoustic frequency. When a_E ranges approximately 0.7 to 1.2, the instability arises with maximum growth rate about the lower hybrid frequency. Note this value to considerably exceed that predicted by the kinetic ion-acoustic instability [12]. The computations for various values of $\cos\varphi$, B_0, and Ar pressures showed that the instability always occurs when a_E lies approximately in the above mentioned range; however, it turns out to be low sensitive to other parameters. Thus, the parametric effect of the pumping field is found to be strong: it substantially modifies the acoustic dispersion and gives rise to the instability with high growth rate.

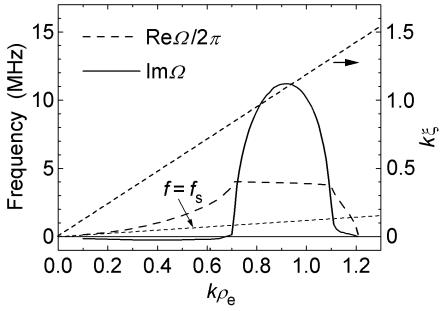

Fig. 11. The LF dispersion in uniform pumping field. p_{Ar} = 5 mtorr; B_0 = 115 G; and $n_0 = 4\times10^{11}$ cm^{-3}

One more possible mechanism for excitation of the LF oscillations is a two-stream instability driven by a dc electron drift current (e.g., [15]). The latter can be induced, for instance, by a ponderomotive force

$$\mathbf{f}_p = -\left\langle m_e (\mathbf{u}\nabla)\mathbf{u} + (e/c)(\mathbf{u} \times \mathbf{B}) \right\rangle, \quad (9)$$

where $\mathbf{u}$ and $\mathbf{B}$ are, respectively, the ac electron velocity and magnetic field, and the angular brackets denote time averaging. This force can result in stationary drift flow of electrons across B_0 with velocity $\mathbf{u}_d = (c/eB_0)(\hat{\mathbf{z}} \times \mathbf{f}_p)$. Though we failed to detect the azimuthal electron drift, computations show that it can be so substantial as to drive the instability. We estimated $\mathbf{u}_d$ with $\mathbf{u}$ and $\mathbf{B}$ computed in linear approximation with use of the code [2]. Figure 12 shows the vector field of $\mathbf{u}_d$ in the central part of plasma cross-section, at z = 20 cm. One can see two off-center, slowly rotating vortices, and a rapid jet that moves through the axis and arises mainly due to centrifugal drift of electrons in the field of ponderomotive force. The jet velocity is 5×10^4 cm/s at I_A = 1 A and thus gets supersonic value at antenna current above a few A. This jet can be efficient driver of ion-acoustic waves.

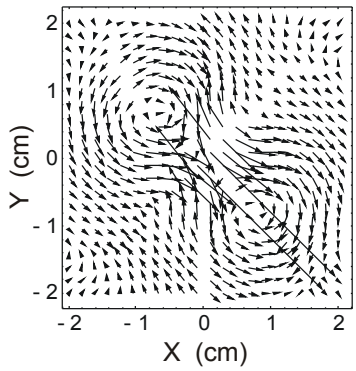

Fig. 12. Vector field of stationary electron flow across B_0 stimulated by ponderomotive force near the axis

The energy density of the LF pulsations was determined by integrating over the low frequency spectrum; its ratio to the plasma thermal energy was found to be of the order of 2×10^{-4}. The maximum density fluctuations were about 10%. It is not yet clear whether this level of turbulence is high enough to provide an effective collision frequency sufficient for the helicon absorption, or it is a sort of by-effect.

3. DISCHARGE IN NONUNIFORM MAGNETIC FIELD

The plasma density in the helicon discharge can increase when the magnetic field is reduced at the antenna location [16-18]. This effect cannot be completely due to better confinement as the total plasma production is strongly increased at the same absorbed power. In our experiment we used, instead of antenna shown in Fig. 1, a double-turn m=0 antenna placed at 6 cm from the left end flange. A naked magnetic probe movable along the axis measured the B_z wave fields and ion saturation current. It was calibrated by using the 8-mm interferometer. The helicon discharge operated at Ar pressure of 5 mTorr and absorbed power of 1 kW.

Figure 13 shows axial distributions of the magnetic field and plasma density. Dashed curves were obtained for the uniform field when all the coils in Fig. 1 were in action. Solid curves correspond to the case when the left

set of coils was turned off and thus the antenna was in the region of decreasing magnetic field. In the latter case, downstream density at z=25 cm turns out to be 6-fold higher at the same absorbed power. Also, the wave amplitude highly exceeds that in the uniform field case.

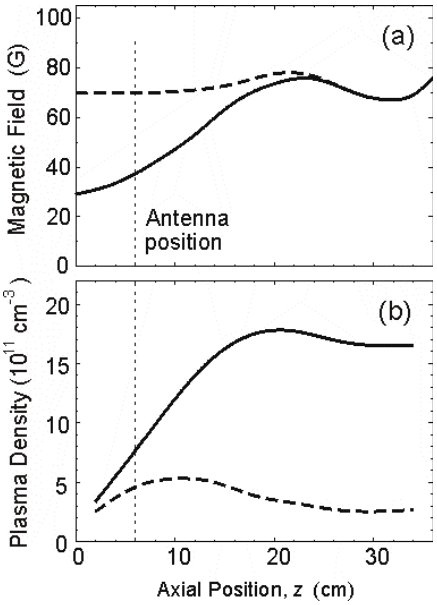

Fig. 13. Dc magnetic field (a) and density (b) profiles

Proposed explanation of density increase is trapping and acceleration of electrons by helicon waves, i.e. again a sort of Landau damping [17]. Our phase measurements showed that in uniform field the helicon phase velocity corresponds to electron energy of 100 eV. In the nonuniform field, it changes from 4 to 15 eV, which is much more favorable for the electron trapping. In this case, additional ion spectral lines with excitation energies ~15 eV were observed. However, our measurements with a flat probe did not detect any fast electrons, and thus the nature of enhanced ionization is not clear. Since the effect is rather strong, some still unknown, basic property of the helicon discharge is thought to be involved.

4. CONCLUSIONS

Several wave effects important for the helicon discharge operation were examined. Modeling experiments with independently prepared plasma allowed us to measure the total antenna impedance as a function of density and magnetic field, for various antenna designs and positions. This is needed for understanding of a short discharge behavior, e.g., the density jumps.

The ion-acoustic turbulence was observed in probe measurements under the helicon antenna. It can be excited as a result of parametric instability or due to azimuthal electron drift induced by a ponderomotive force. Measured total energy of the acoustic turbulent pulsations seems to be insufficient for the helicon absorption.

Plasma production was shown to strongy increase in nonuniform magnetic field. Further experiments are needed for revealing the physical reason of enhanced plasma production.

REFERENCES

1. F.F.Chen and R.W.Boswell. *IEEE Trans. Plasma Sci.* **25** (1997) 1245.
2. V.F.Virko, G.S.Kirichenko and K.P.Shamrai. *Plasma Sources Sci. Technol.* **11** (2002) 10.
3. K.P.Shamrai. *Plasma Sources Sci. Technol*. **7** (1998) 499.
4. K.K.Chi, T.E.Sheridan and R.W.Boswell. *Plasma Sources Sci. Technol*. **8** (1999) 421.
5. K.P.Shamrai, V.F.Virko, H.-O.Blom et al. *J. Vac. Sci Technol.* A **15** (1997) 421.
6. J.P.Rayner and A.D.Cheetham. *Plasma Sources Sci. Technol.* **8** (1999) 79.
7. T.Shoji, Y.Sakawa, S.Nakazawa et al. *Plasma Sources Sci. Technol*. **2** (1993) 5.
8. F.F.Chen and G.Chevalier. *J. Vac. Sci. Technol.* A **10** (1992) 1389.
9. K.P.Shamrai and V.B.Taranov. *Plasma Sources Sci. Technol.* **5** (1996) 474.
10. L.I.Grigor'eva, V.L.Sizonenko, B.I.Smerdov, et al. *Zh. Eksp. Teor. Fiz*. **60** (1971)605.
11. M.Porcolab, V.Arunasalam and R.A.Ellis. *Phys. Rev. Lett.* **29** (1972) 1438.
12. A.I.Akhiezer, V.S.Mikhailenko and K.N.Stepanov. *Phys. Lett*. A **245** (1998) 117.
13. N.M.Kaganskaya,.M.Krämer and V.L.Selenin. *Phys. Plasmas* **8** (2001) 4694.
14. Yu.M. Aliev, V.P. Silin and C. Watson. *Zh. Eksp. Teor. Fiz*. **50** (1966) 943
15. R.L.Stenzel. *Phys. Fluids* B **3** (1991) 2568.
16. G.Chevalier and F.F.Chen. *J. Vac. Sci. Technol.* A **11** (1993)1165.
17. X.M.Guo, J.Sharer, Y.Mouzouris and L.Louis. *Phys. Plasmas* **6** (1999) 3400.
18. O.V.Braginskij, A.N.Vasil'eva and A.S.Kovaljov. *Fiz. Plazmy* **27** (2001) 741.

ХВИЛЬОВІ ЯВИЩА В ГЕЛІКОННІЙ ПЛАЗМІ

В.Ф. Вірко, Г.С. Кириченко, К.П. Шамрай

Представлено результати експериментальних та теоретичних досліджень хвильових процесів у густій плазмі, які збуджуються ВЧ антенами різних конструкцій в діапазоні геліконних частот. Експерименти проведено в комбінованому ЕЦР-геліконному джерелі плазми. Виявлено, що виміряна багатопікова структура залежності поглинання від густини плазми задовільно узгоджується з результатами обчислень і пов'язана зі збудженням стоячих поздовжніх мод. Зі збільшенням ВЧ потужності досліджено перехід до самостійного геліконного розряду. В чисто геліконному розряді виміряні спектри шумових коливань, які включають НЧ смугу з шириною порядку 1 МГц та ряд ВЧ смуг поблизу основної частоти та її гармонік. Збудження НЧ коливань має поріг по потужності, тобто відбувається параметричним чином, а також по магнітному полю. Ці коливання ідентифіковано з іонно-звуковими хвилями, що розповсюджуються по азимуту у напрямку обертання електронів. Їхні кореляційні довжини зменшуються зі зростанням магнітного поля, а інтенсивність різко збільшується безпосередньо під антеною. Обчислення показують, що в умовах експерименту генерація звуку можлива як за рахунок параметричної нестійкості, так і внаслідок дрейфової течії електронів в полі пондеромоторної сили. Досліджено також геліконний розряд в неоднорідному магнітному полі та виявлено різке зростання генерації плазми порівняно з випадком однорідного поля.

ВОЛНОВЫЕ ЯВЛЕНИЯ В ГЕЛИКОННОЙ ПЛАЗМЕ

В.Ф. Вирко, Г.С. Кириченко, К.П. Шамрай

Представлены результаты экспериментальных и теоретических исследований волновых процессов в плотной плазме, возбуждаемых ВЧ антеннами различных конструкций в диапазоне геликонных частот. Эксперименты проведены в комбинированном ЭЦР-геликонном источнике плазмы. Обнаружено, что наблюдаемая многопиковая структура зависимости поглощения от плотности плазмы удовлетворительно согласуется с результатами вычислений и связана с возбуждением стоячих продольных мод. При увеличении ВЧ мощности исследован переход к самостоятельному геликонному разряду. В чисто геликонном разряде измерены спектры шумовых колебаний, которые включают НЧ полосу с шириной порядка 1 МГц и набор ВЧ полос вблизи основной частоты и ее гармоник. Возбуждение НЧ колебаний имеет порог по мощности, т.е. происходит параметрическим образом, а также по магнитному полю. Эти колебания идентифицированы с ионнозвуковыми волнами, распространяющимися по азимуту в направлении вращения электронов. Их корреляционная длина уменьшается с ростом магнитного поля, а интенсивность резко возрастает непосредственно под антенной.. Вычисления показывают, что в условиях эксперимента генерация звука возможна как за счет параметрической неустойчивости, так и вследствие дрейфового течения электронов в поле пондеромоторной силы. Исследован также геликонный разряд в неоднородном магнитном поле и обнаружено резкое возрастание генерации плазмы в сравнении со случаем однородного поля.